# Separation of the Earthquake Tomography Inverse Problem to Refine Hypocenter Locations and Tomographic Models: A Case Study from Central Oklahoma


Toth, C.R.[1] Chen, C.[1] Holland, A.A.[2]

[1] University of Oklahoma, Norman; [2] Oklahoma Geological Survey


## Abstract


The tomographic inverse problem is sensitive to both the velocity anomaly distribution and hypocenter origins. By using an inversion approach to solve for both hypocenter origins and velocity structure, additional unconstrained dampening parameters must be set to run the joint inversion. Each dampening parameter has a range of reasonable values, so the more inversion parameters that must be set to run the inversion increases the ambiguity in the final model. Furthermore, since the tomographic modeling and 3D hypocenter location steps both benefit greatly from grid searching and analysis trade-off curves, determining the range of reasonable values for each of the inversion parameters can become an increasingly difficult problem in itself as the number of dampening and model parameters increase. For these reasons, we separate the hypocenter location process from the tomographic inversion and run these steps iteratively.

Oklahoma has seen a dramatic increase in seismicity over the last several years. Two pockets of seismicity account for much of the increase, the first being the eastern Oklahoma City swarm, and the second being the Wilzetta Fault rupture. The data used in this study were obtained from a deployment of 174 seismometers spanning the 50 kilometers between these two seismically active areas, recording eight earthquakes. Approximately 1,500 P and S travel times for direct and refracted rays were used to constrain 3D tomographic modeling using FMTomo (Rawlinson, 2006) and to locate the hypocenters in the resulting 3D tomographic model in NonLinLoc (Lomax et al, 2000).


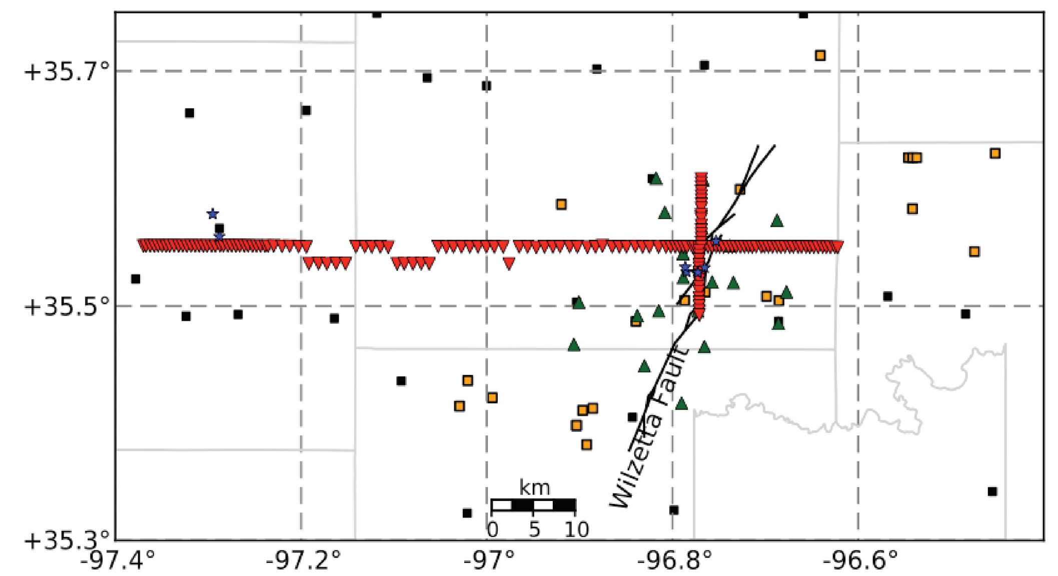


**Figure 1:** Geometry of the seismic array used in this study. Blue stars: earthquake locations; Black lines: Wilzetta Fault (Joseph, 1987); Grey lines: county boundaries; Green Triangles: stations used in this study and in Keranen et al (2013); Inverted red triangles: 156 additional stations used in this study; Orange squares: locations of sonic logs; Black squares: small towns.

## Velocity Model

An initial 1D velocity model (figure 2) was developed by digitizing and averaging compressional sonic logs for the 22 closest wells to the Wilzetta Fault to constrain the shallowest ~2km of the crust (figure). Deeper velocities were constrained by analyzing surface wave dispersion curves (Robert Herman, personal communication, 2012).

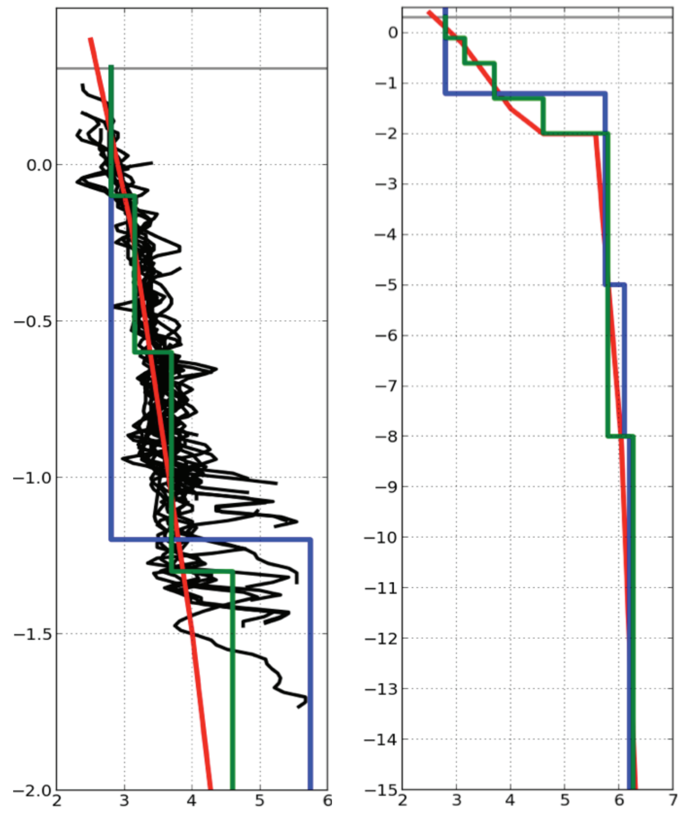

**Figure 2: Left:** Velocity models and sonic logs from the Wilzetta Fault area down to 2km deep, the top of crystalline basement (Luza and Lawson, 1981).

**Right:** Velocity models down to 15 km.

*Blue*: final 1D model used in Keranen et al (2013).
*Red*: gradient-based starting model used in this study (input for NonLinLoc).
*Green*: discrete-layer starting model used in this study (input for HypoDD2.1b and FMTomo).
*Black*: Smoothed sonic logs.
*Grey*: Average station elevation.

## Tomographic Inversion

Locations were initially generated in NonLinLoc. These locations were input into FMTomo, where a highly-dampened hypocenter inversion was enabled to allow the earthquakes to move slightly in a changing velocity field.

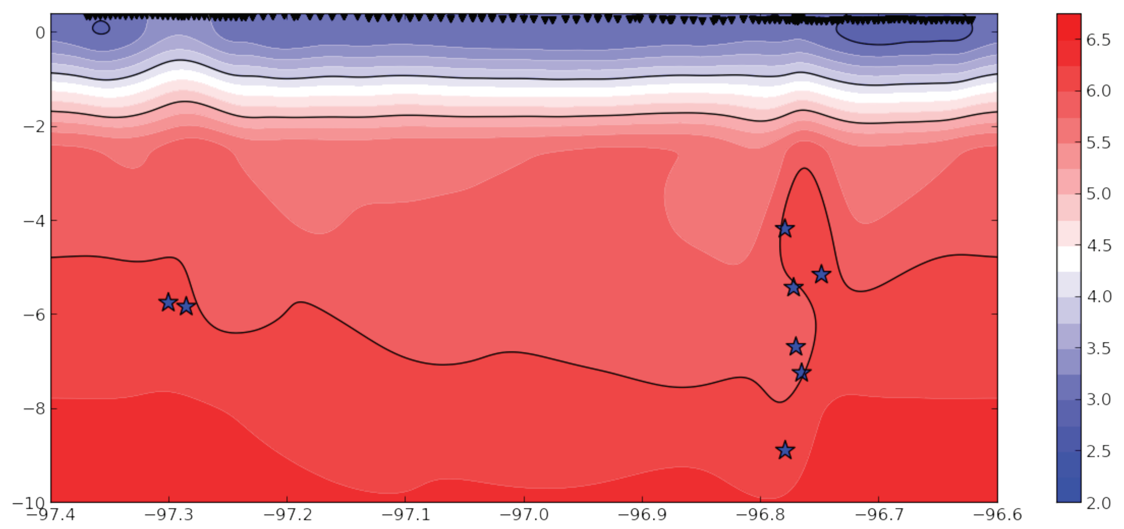

**Figure 3:** Cross-section under latitudinal reciever line. final model misfit is 76ms.
Blue start: Earthquakes
Black triangles: receivers

## Model Verification

Dues to the limited number of recorded events, the inversion's sensitivity to each earthquake, especially in regards to the precision of hypocenter locations, was tested. Models were run using subsets of 6 earthquakes, shown in figures 4 and 5. Another model including an additional 38 well-recorded earthquakes from the OGS regional earthquake catalog is shown in figure 6. Additionally, for each of these comparison models, the Mean Absolute Percent Error (MAPE) is calculated for the entire 3D volume.

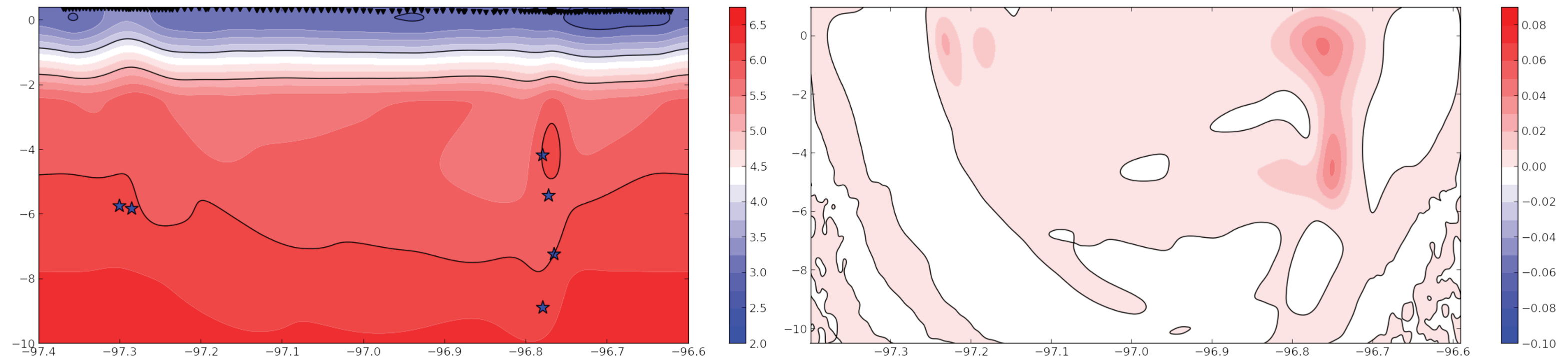

**Figure 4: Left:** Tomographic model generated by omitting 25% of the data that was used to generate figure 3. Cross-section through same coordinates as in figure 3. **Right:** Cross-section showing the percent difference between this velocity model and the model generated with all the data. Total MAPE through the entire volume is 0.08%.

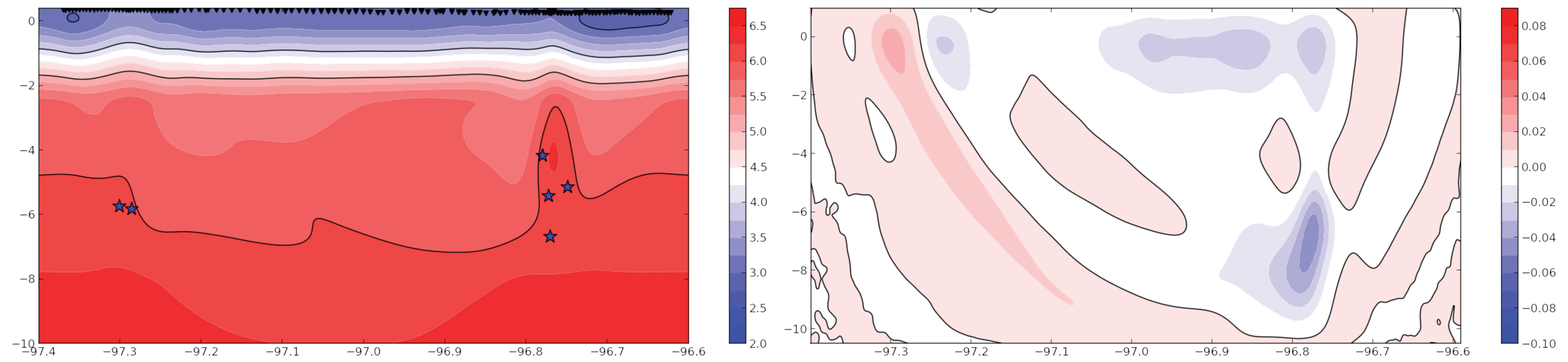

**Figure 5: Left:** Tomographic model generated by omitting a different 25% of the data. Cross-section through same coordinates as in figure 3. **Right:** Cross-section showing the percent difference between this velocity model and the model generated with all the data. Total MAPE through the entire volume is 0.12%.

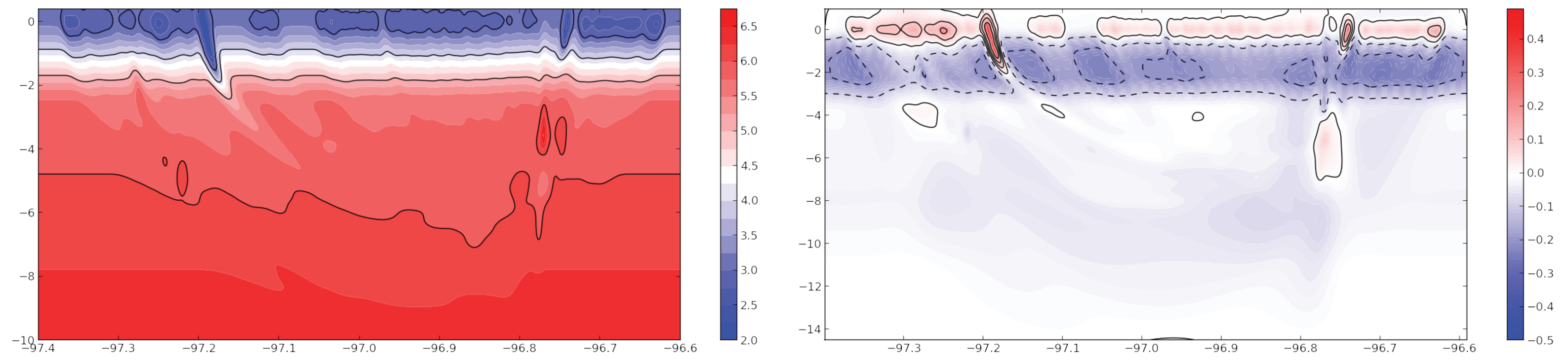

**Figure 6: Left:** Tomographic model generated by adding the 38 earthquakes captured on the most local temporary stations in the study area. Cross-section through same coordinates as in figure 3. **Right:** Cross-section showing the percent difference between this velocity model and the model generated with all the data. Total MAPE through the entire volume is 4.5%.

## 3D Hypocenter Relocations

The 3D velocity model shown in figure 3 was used in NonLinLoc to locate ~100 well-recorded aftershocks of the Wilzetta Fault rupture of 2011. Of these events, only ~7.5% were located in the sedimentary column (i.e. < 2km deep).

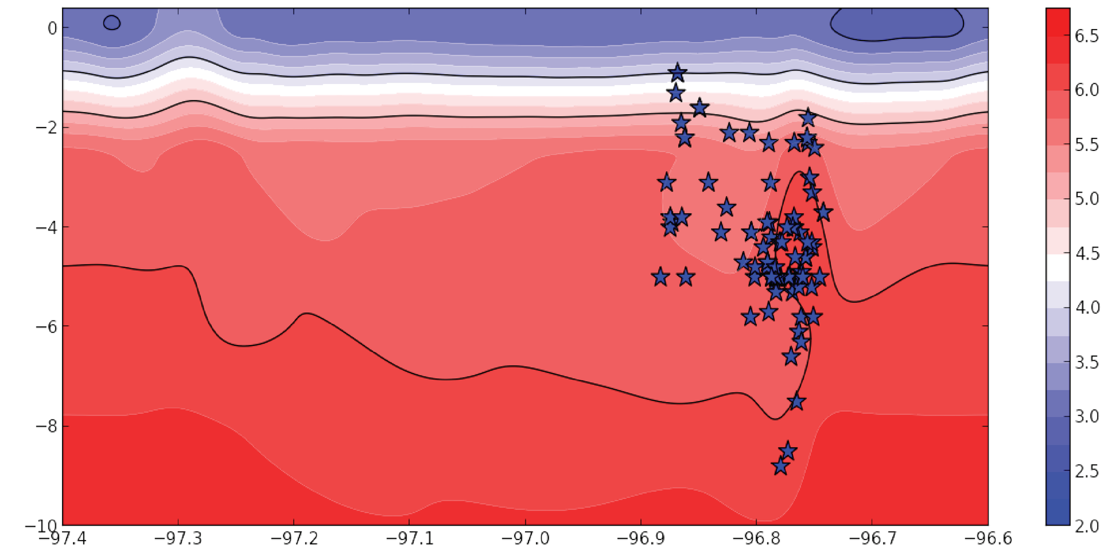

## Discussion

- The basement structure in the Wilzetta Fault area appears to be more complicated than originally thought.

- The locations here are significantly deeper than those reported in Keranen (2013).

## References


Keranen, K. M., Savage, H. M., Abers, G. A., and Cochran, E. S., 2013, Potentially induced earthquakes in Oklahoma, USA: Links between wastewater injection and the 2011 Mw 5.7 earthquake sequence: Geology, v. 41, no. 6, p. 699-702.

Lomax, A., Virieux, J., Volant, P., and Berge-Thierry, C., 2000, Probablistic Earthquake Location in 3D and Layered Models, in Thurber, C. H., Raabinowitz, N., ed., Advances in Seismic Event Location: Boston, MA, Kluwer Academic Publishers, p. 101-134.

Luza, K. V., and Lawson, J. E., 1981, Seismicity and Tectonic Relationships of the Nemaha Uplift, part III: Oklahoma Geological Survey Special Publication, v. 81-3, 70p.

Rawlingson, N., Reading, A. M., and Kennett, B. L. N., 2006, Lithospheric structure of Tasmania from a novel form of teleseismic tomography: J. Geoph. Res., v. 111, no. B02301, p. 1-21.